EUROPHYSICS LETTERS 1 June 2006

Europhys. Lett., **74** (5), pp. 771–777 (2006)
DOI: 10.1209/epl/i2006-10028-6

Scattering-induced dynamical entanglement and the quantum-classical correspondence

M. Lombardi and A. Matzkin

Laboratoire de Spectrométrie physique (CNRS Unité 5588), Université Joseph-Fourier Grenoble-1 - BP 87, 38402 Saint Martin d'Hères, France

received 9 January 2006; accepted in final form 30 March 2006
published online 12 April 2006

PACS. 03.67.Mn – Entanglement production, characterization, and manipulation.
PACS. 05.45.Mt – Quantum chaos; semiclassical methods.
PACS. 34.60.+z – Scattering in highly excited states (*e.g.*, Rydberg states).

Abstract. – The generation of entanglement produced by a local potential interaction in a bipartite system is investigated. The degree of entanglement is contrasted with the underlying classical dynamics for a Rydberg molecule (a charged particle colliding on a kicked top). Entanglement is seen to depend on the structure of classical phase-space rather than on the global dynamical regime. As a consequence, regular classical dynamics can in certain circumstances be associated with higher entanglement generation than chaotic dynamics. In addition, quantum effects also come into play: for example, partial revivals, which are expected to persist in the semiclassical limit, affect the long-time behaviour of the reduced linear entropy. These results suggest that entanglement may not be a pertinent universal signature of chaos.

Entanglement, *i.e.* the nonseparability intrinsic to composite systems, is one of the most peculiar features of the quantum world. In its most popular form, found for example in the original EPR proposal [1], the entanglement is of geometrical nature. However any usual potential interaction between two particles can generically lead to entanglement, provided several quantum states are accessible to both particles. The study of such dynamical entanglement is particularly interesting for systems which possess a classical counterpart. Indeed as is well known [2], such systems can be investigated with semiclassical tools, allowing to interpret the quantum dynamics in terms of classical properties. Recent investigations have been focusing on the relation between the generation of entanglement and the underlying classical dynamics. Initial work in spin-boson systems [3] and in coupled kicked tops [4] suggested that chaotic dynamics generate more and faster entanglement. This claim was subsequently revised [5,6] and efforts are now being made to derive universal relations ruling the generation of entanglement irrespective of system specifics. Different approaches based on perturbation expansions [5,7,8], Random Matrix theory [9,10] and semiclassical methods [11,12] have been proposed. In particular it was shown and verified [11,13] that entanglement generated from initial Gaussian states averaged over configuration space depends on the global classical dynamical regime. However, contrarily to the well-established quantum-classical correspondence for spectral statistics and large-scale fluctuations [14], it is still not clear to what extent an analog universal correspondence exists for dynamical entanglement production; for example,

the dependence of entanglement on non-classical features like the type of initial states [7] or their spectral width [9] has been put forward.

In this work we study the generation of entanglement for a real system which possesses an unambiguous classical counterpart. This will be done by employing a bipartite system where entanglement is produced by a *local* interaction, viz. the particles interact via a short-range scattering potential. Our model enables more stringent tests on the transition to chaos than usual models in which this transition depends essentially on a single coupling parameter and occurs relatively uniformly on the whole phase space. Indeed we use a system in which a second essential parameter, the resonance parameter, produces global changes of the phase-space picture, changing dramatically the coupling necessary to induce chaos. We will see that the underlying classical dynamics is reflected in the generation of entanglement. However, this dependence involves particular features in the structure of phase-space rather than the global dynamical (chaotic or regular) regimes. Quantum effects also come into play, particularly at long times.

The system investigated here is a Rydberg molecule. Simply stated, a Rydberg molecule is composed of two parts: a highly excited electron on the one hand, and a compact ionic molecular core, containing the nuclei and the tightly bound other electrons on the other. Most of the time, the outer electron and the core are spatially well separated: the core rotates freely with angular momentum $\boldsymbol{N}$ and energy $E_N^+ \propto N^2$, whereas the outer electron senses a pure Coulomb field. Its orbital angular momentum $\boldsymbol{L}$ is fixed in space. Seen in the molecular frame, $\boldsymbol{L}$ turns around the $\boldsymbol{N}$ axis (see fig. 1(a, e)). However, the outer electron periodically scatters on the molecular core. Classically, the electron is kicked by the rotating core. This kick results in a change in the direction of $\boldsymbol{L}$ by $\Delta\varphi$, the deflection angle of the plane of the classical Kepler orbit. $\boldsymbol{N}$ adjusts accordingly, since the total angular momentum $\boldsymbol{J} = \boldsymbol{L} + \boldsymbol{N}$ is conserved. The conservation of $\boldsymbol{L}$ and the cylindrical symmetry of the core implies that $\Delta\varphi = k\cos\theta$, where k gives the strength of the kick. A negligibly small kick yields regular dynamics. This is visualised in a Poincaré surface of section obtained by plotting the position of $\boldsymbol{L}$ after each kick (fig. 1) [15]. As k increases, two cases must be distinguished. In the generic case (figs. 1(b)-(d)) chaos appears and invades rapidly the whole phase space until the last islands of regularity disappear. Things are different in the resonant case. Resonances appear when the orbital period of the electron T_e and the rotational period of the core T_0 are commensurate, so resonances are nongeneric. Chaos is inhibited and finally appears along the separatrix (figs. 1(f)-(h)) for much higher values of the coupling k. Such resonances are known to modify the spectrum of small Rydberg molecules, giving rise to the stroboscopic effect experimentally observed on Na_2 [16].

In quantum-mechanical terms the collision couples the electron and core dynamics and induces phase-shifts in the wave function of the outer electron. In the absence of the core-electron interaction, the Hamiltonian H_0 is separable and the eigenstates are given by the product state

$$\phi_N(E, r) = f_L(E - E_N^+, r) \otimes |N\rangle\,, \tag{1}$$

where E is the total energy, $|N\rangle$ the state of the core and f_L the radial Coulomb function of the electron whose energy is $\epsilon_N = E - E_N^+$ [17]. The total Hamiltonian $H = H_0 + V$ includes the core-electron interaction potential V. The eigenstates are given from scattering theory by

$$\psi(E, r) = \sum_N Z_N(E)\,[I + G_0(E)K]\,\phi_N(E, r), \tag{2}$$

where G_0 is the Green's function, Z_N are expansion coefficients and K is the scattering matrix, whose elements $K_{N'N}$ are related to the transition probability amplitude between states ϕ_N

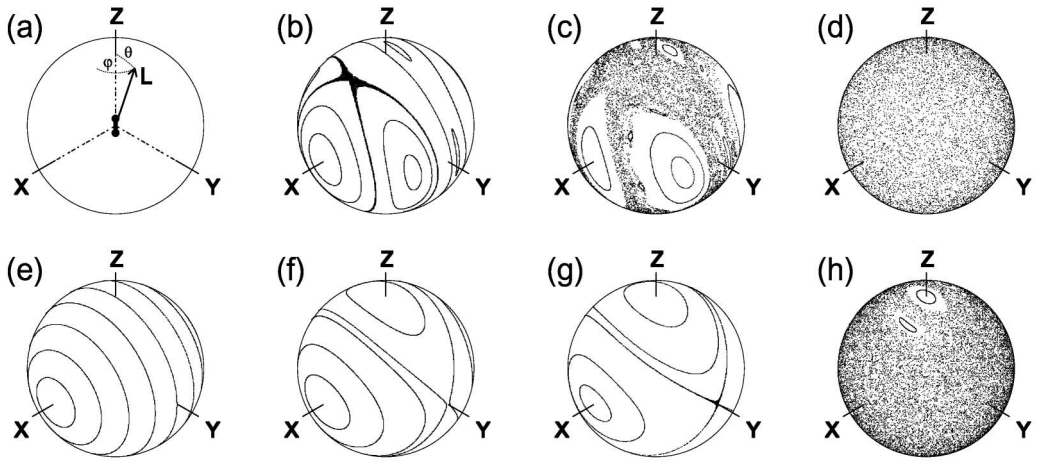

Fig. 1 – Poincaré surfaces of section in the molecular frame. (a) defines the angles θ and φ for a given position of $\boldsymbol{L}$ on the sphere. The core axis is along OZ and $\boldsymbol{N}$ along OX. (e) shows the $k = 0$, no-coupling situation, valid for all values of T_e and T_0; one sees only the free apparent rotation of $\boldsymbol{L}$ around the core angular momentum $\boldsymbol{N}$, describing circles. On a given circle, the modulus N is constant, but it varies from circle to circle. (b)-(d) and (f)-(h): generic case (top row) and resonant ($T_e = T_0$) case (bottom row) for increasing coupling. (b) and (f): $k = 0.25$, (c) and (g): $k = 0.5$, (d) and (h): $k = 10$. Note that in the generic case, circles (tori in whole phase space) which correspond to low rational values of the returning times of electron and core open resonant islands: values 2 and 4 appear clearly in (b). Chaos appears along the corresponding unstable manifolds and invades rapidly the whole phase-space until the last islands of regularity disappear (image (d)). In the resonant case a very large couple of resonance islands appears around the $\pm OZ$ axis (the top one is visible in (f)-(h)), with a separatrix starting from the $\pm OY$ axis.

and $\phi_{N'}$ due to the collision. From eq. (2) it is apparent that an eigenstate is given by a superposition of core states with rotational number N, each core state being associated with an outer electron having an energy ϵ_N. The relation between the quantum and classical pictures is simpler [15] when expressed in the molecular frame, where K has only diagonal elements $\tan\delta_\Lambda$. The phase-shifts δ_Λ only depend on the coupling between $\boldsymbol{L}$ and the molecular axis. $\Lambda = L\cos\theta$ is the projection of $\boldsymbol{L}$ on this axis and the classical deflection angle is related to the quantum phase shifts by

$$\Delta\varphi = 2\frac{\partial\delta_\Lambda}{\partial\Lambda} = k\frac{\Lambda}{L}. \tag{3}$$

The first equality is a very general result stemming from the semiclassical approximation to scattering theory [18] and is valid to first order in $\hbar$, whereas the last term follows from the functional relation $\delta_\Lambda(k)$ chosen in this work which turns out to be verified for typical diatomic molecules.

To quantify entanglement we will employ the linear entropy S_2, as has been done in most previous works [3, 5–12]. Indeed for bipartite systems S_2 behaves as other measures of entanglement [19] while being convenient to compute. The linear entropy associated with the reduced density matrix describing the electron is given by

$$S_2 = 1 - \mathrm{Tr}_e\rho_e^2, \tag{4}$$

where $\rho_e = \mathrm{Tr}_c\rho$ and as usual Tr_c (Tr_e) refers to averaging over the core (electron) degrees of freedom. We first determine the degree of entanglement of stationary states. This is done

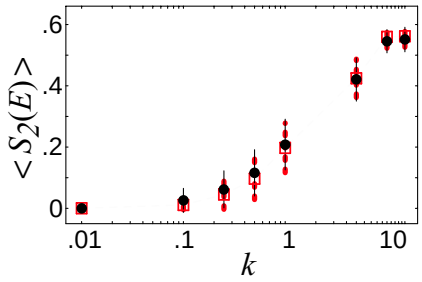

Fig. 2 – (Colour on-line) Average linear entropy for generic (red/gray boxes) and resonant (black dots) states ($T_e = T_0$), shown for different values of k. The rms is also shown as red dashed (generic) and solid (resonant) error bars.

by calculating $\rho(E) = |\psi(E)\rangle\langle\psi(E)|$ over an energy range for which the classical dynamics does not vary appreciably. The values $L = 2$ and $J = 10$ adopted in this work correspond to experimentally accessible values for diatomic molecules such as Na_2. With these values and taking into account symmetry requirements, three rotational states are accessible to the core $N = 8$, 10, 12 (classically, $8 \leq N \leq 12$). Hence in a typical eigenstate (2) three core-electron states are entangled. The mean entropy $\langle S_2(E)\rangle$ for stationary states is shown in fig. 2 as a function of the coupling constant k. The curves for the generic and resonant cases are very close despite phase-space being substantially different for most values of k. On average, the potential interaction entangles at least as efficiently when the underlying classical dynamics is mostly regular rather than mainly chaotic. Note that the rms is small for the regular and totally chaotic regimes and larger in the mixed phase-space situation and that the linear entropy saturates in both the generic and resonant cases only for large k: $\langle S_2(E)\rangle$ approaches its upper limit 2/3 corresponding to a maximally mixed state.

We next determine the time-dependent generation of entanglement from an initial product state. At $t = 0$ we take the wave function of the electron to be radially localised at the outer turning point r_{tp}, several thousand atomic units away from the core, and we take the core to be in the rotational state $|N_0\rangle$, so that

$$\psi(t = 0, r) = F_{loc}(r \approx r_{tp}) \otimes |N_0\rangle\,. \tag{5}$$

The mean energy of the radial wavepacket F_{loc} is $\epsilon_0 = E_0 - E^+_{N_0}$ and T_e is the period of the corresponding Kepler orbit. At $t \approx T_e/2$ the wavepacket scatters off the core and the wave function is given by a *superposition* of radial wavepackets moving outward, each associated with a core in a given rotational state $|N\rangle$. At $t \approx T_e$ each of the radial wavepackets has reached the outer turning point and starts going back towards the core. The core-electron interaction then takes place again at $t \approx 3T_e/2$ resulting in further entanglement change. As t increases the wavepackets tend to spread radially resulting in a continuous core-electron interaction. These features appear in the time dependence of the linear entropy $S_2(t)$, obtained from eq. (4) by tracing out the core degrees of freedom from the total density matrix $|\psi(t)\rangle\langle\psi(t)|$.

For short times $S_2(t)$ is shown in fig. 3, for $N_0 = 8$ and for 3 different values of the coupling k. In the generic case, for small t and not too large k, S_2 is seen to increase linearly in steps, reflecting the discrete times core-electron interaction, and then appears to saturate (but see below). In the resonant case, the linear entropy also increases on average linearly but displays oscillations. Indeed, a semiclassical approximation for the short-time behaviour of the purity $\mathrm{Tr}_e\rho_e^2$ predicts that $S_2(t_C) \propto k^2 t_C$. This result, valid only for the collision times $t_C =$

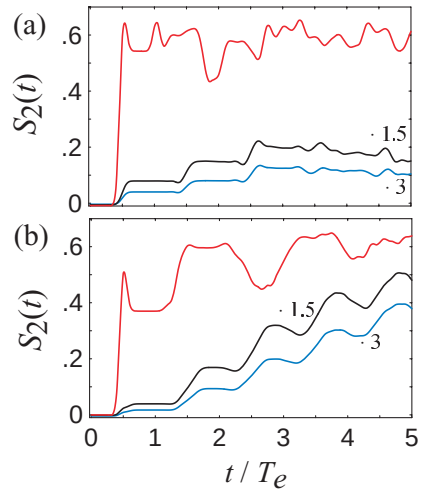

Fig. 3 – (Colour on-line) Short-time variation of the linear entropy for different values of the coupling strength; t is given in units of the Kepler period T_e. (a) Generic phase-space, from top to bottom $k = 10$ (red), 0.5 (black) and 0.25 (blue). The $k = 0.25$ ($k = 0.5$) curve is multiplied by a factor 3 (1.5). (b) Same as (a) for the resonant case $T_e = T_0$.

$(2m + 1)T_e/2$, is obtained in the stationary phase approximation by neglecting correlations between electron orbits built on different core rotational states. This linear behaviour agrees with the prediction of [12]. The k^2-dependence comes from the semiclassical amplitudes, and the linear variation in t from the fact that these amplitudes are conserved. The oscillations of S_2 observed in the resonant case arise from the coherent projection of the motion of the outer electron. It is in this sense a kinematical effect, since no such behaviour is to be found in the wave function or in the probability flux. By expanding the core energies to first order, the purity is seen to depend on terms of the form

$$\sum_{NN'} |e^{-2i\pi t\left[(N-N')/T_0\right]} \sum_{\epsilon(N)\epsilon'(N')} e^{-i(\epsilon-\epsilon')t} Z_N(E) Z_{N'}(E') \left\langle F_L(\epsilon'(N'))\right| F_L(\epsilon(N))\rangle\,|^2, \qquad (6)$$

where $\epsilon_N = E - E_N^+$ and $F_L(\epsilon, r)$ are radial functions on the energy shell (*i.e.* a combination of regular and irregular Coulomb functions with effective phase shifts depending on the scattering matrix K). These functions form an overcomplete basis and are not orthogonal in ϵ. In the generic case the nondiagonal terms in the second sum are generally small and uncorrelated. However, at resonance both exponentials are in phase (since $\epsilon - \epsilon' \approx 2m\pi/T_0$) and the correlations between nondiagonal terms are enhanced, because the resonance imposes a greater similarity of certain corresponding eigenstates (2) [15].

The long-time behaviour of the entanglement production is shown in fig. 4. In the generic case, $S_2(t)$ is on average very low for $k = 0.25$ (corresponding to classically regular phase space), higher for $k = 0.5$ (mixed phase-space) and nearly maximal for $k = 10$ (chaotic phase-space). Periodic recoherences are visible for small k. Although revivals are expected when phase-space is regular and the dimensionality of the Hilbert space is low, we point out that the same observations have been made for considerably larger angular momenta closer to the semiclassical limit [20]. The characteristic periods of recoherence involve the revival times T_0^{rev} and T_e^{rev} of the core rotation and the electron orbit. The former readily appears by carrying the expansion in E_N^+ in eq. (6) to second order. The latter follows by remarking

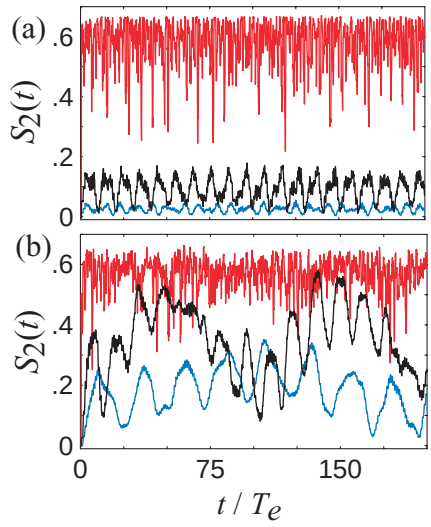

Fig. 4 – Same as fig. 3 for longer times; the curves for $k = 0.25$ and $k = 0.5$ are *not* multiplied by any factor. The oscillations visible for these curves depend on the revival time of the partial correlation functions. For example, in (b) for $k = 0.5$, two scales are visible corresponding to $T_e^{rev}(N = 10)$ and the longer $T_e^{rev}(N = 12)$.

that the second sum in eq. (6) is the cross-correlation function between parts of the wave function belonging to different superposition alternatives (*i.e.* different scattering channels). Alternatively, it can be shown [21] that the purity is bounded from below by correlation functions which vary according to the revival times. Note that the revivals have no classical counterpart. In the resonant case the long-range oscillations can be dramatically enhanced by the commensurate time scales (in addition to $T_0 = T_e$, we have $T_0^{rev} \approx 2T_e^{rev}$) and the similarity of the eigenfunctions which makes the cross-correlations to be very large. The consequence is that the curves for k values corresponding to different underlying classical dynamics may cross.

These results indicate that the behaviour of the linear entropy is not simply connected to the classical regime, but also depends on the structure of phase-space. Indeed the entanglement production is considerably *higher* in the resonant case despite classical phase-space being much more *regular* (compare figs. 1(c) and (g) with their respective curves in fig. 4). This behaviour can be ascribed to the large values of the cross-correlations, which are ultimately due to the fact that at resonance $\boldsymbol{L}$ appears to move around the core axis OZ, and therefore its projection on $\boldsymbol{N} = OX$ (and thus the possible values of N^2) tends to spread. Classically, resonances modify the structure of phase-space by the appearance of a fixed point on the OZ core axis, which is visible in the Poincaré surfaces of section (fig. 1). In quantum-mechanical terms N is then not well defined and thus the wave functions are mixed in $|N\rangle$ even for small kick strengths. In the generic case however these mixings can only take place for large values of the coupling, corresponding to chaotic dynamics.

To conclude we have investigated the generation of entanglement induced by a potential interaction in a bipartite system, a Rydberg molecule. By and large chaotic classical dynamics is associated with more and faster entanglement because the scattering particles explore larger portions of phase-space leading quantum-mechanically to superpositions. But chaos is not necessarily the most efficient way to ensure that the relevant part of phase-space leading to

superpositions (in our system the rate of inelastic scattering) is explored with a large classical amplitude: this is why a dynamical effect such as resonances generate higher entanglements despite classical phase-space being mostly regular. On the other hand, it has been shown [11,13] that for weak coupling the purity does depend on the global dynamical regime when a given type of initial state is averaged over all the possible initial positions. But it is also known that the average entanglement is sensitive to the form of the initial state [7]. From a general standpoint we would like to point out that the universal relations between quantum fluctuations and average classical phase-space properties are known to be spoiled by nongeneric families of periodic orbits [22] that are expected to proliferate in systems (such as Rydberg systems) that are strongly coupled by potential scattering [23] which is here the generator of entanglement.

* * *

We are grateful to T. H. Seligman (UNAM, Cuernavaca, Mexico) for fruitful discussions.

REFERENCES

[1] Einstein A., Podolsky B. and Rosen N., *Phys. Rev.*, **47** (1935) 777.
[2] Brack M. and Bhaduri R. K., *Semiclassical Physics* (Addison-Wesley, Reading, Mass.) 1997.
[3] Furuya K., Nemes M. C. and Pellegrino G. Q., *Phys. Rev. Lett.*, **80** (1998) 5524.
[4] Miller P. A. and Sarkar S., *Phys. Rev. E*, **60** (1999) 1542.
[5] Fujisaki H., Miyadera T. and Tanaka A., *Phys. Rev. E*, **67** (2003) 066201.
[6] Novaes M. and de Aguiar M. A. M., *Phys. Rev. E*, **70** (2004) 045201(R).
[7] Demkowicz-Dobrzanski R. and Kus M., *Phys. Rev. E*, **70** (2004) 066216.
[8] Angelo R. M. and Furuya K., *Phys. Rev. A*, **71** (2005) 042321.
[9] Gorin T. and Seligman T. H., *Phys. Lett A*, **309** (2003) 61.
[10] Bandyopadhyay J. N. and Lakshminarayan A., *Phys. Rev. E*, **69** (2004) 016201.
[11] Jacquod Ph., *Phys. Rev. Lett.*, **92** (2004) 150403.
[12] Znidaric M. and Prosen T., *Phys. Rev. A*, **71** (2005) 032103.
[13] Petitjean C. and Jacquod Ph., Eprint (2005) quant-ph/0510157.
[14] Haake F., *Quantum Signatures of Chaos* (Springer, Berlin) 2001.
[15] Dietz B., Lombardi M. and Seligman T. H., *Ann. Phys.*, **312** (2004) 441; Lombardi M. *et al.*, *J. Chem. Phys.*, **89** (1988) 3479.
[16] Labastie P. *et al.*, *Phys. Rev. Lett.*, **52** (1984) 1681; Chang E. S. *et al.*, *J. Chem. Phys.*, **111** (1999) 6247.
[17] The angular part of the electron wave function is contained in the compound notation $|N\rangle$ due to the coupling of angular momenta. This "geometrical entanglement" plays no role in this work which focuses on the superpositions in $\boldsymbol{N}^2$ and not in the relative orientations of the angular momenta.
[18] Newton R. G., *Scattering Theory of Waves and Particles* (Springer, New York) 1982, Chapt. 18.
[19] Berry D. W. and Sanders B. C., *J. Phys. A*, **36** (2003) 12255.
[20] Lombardi M. and Matzkin A., in preparation.
[21] Prosen T., Seligman T. H. and Znidaric M., *Phys. Rev. A*, **67** (2003) 062108.
[22] Hönig A. and Wintgen D., *Phys. Rev. A*, **39** (1989) 5642; Sieber M. *et al.*, *J. Phys. A*, **26** (1993) 6217.
[23] Matzkin A. and Monteiro T. S., *J. Phys. A*, **37** (2004) L225.